In many of the holographic images recorded of different states of the shock wave, there was a strong spanwise variation of the fringe pattern. Since the formation and localization of that pattern depends upon the shock slope, curvature, the positional variation in shock strength, and the time variation of these quantities, there is some evidence of a spanwise variation in the space- and time-dependent properties of the shock wave.

## Conclusions

The results, based on observations of holographic images, reveal a relatively narrow two-dimensional shock surface moving over airfoils which are driven to simulate transonic torsional flutter. However, some of these same holograms revealed a spanwise variation in the shock properties. This latter behavior warrants further investigation for it could have important ramifications concerning the use of experimental results from driven transonic cascades of this type. This exploratory study also indicates the feasibility of using diffuse-illumination, rapid double-exposure holographic interferometry for visualization of the shock structure in a transonic flutter cascade.

## References

[1] Riffel, R. E. and Rothrock, M. D., "Experimental Determination of Unsteady Blade Element Aerodynamics in Cascades, Vol. 1: Torsion Mode Cascade Final Report," Detroit Diesel Allison Div., General Motors Corp., Indianapolis, Ind., Rept. EDR-10119-VOL-1, June 1980 (also NASA CR-159831).

[2] Boldman, D. R. and Buggele, A. E., "Wind Tunnel Tests of a Blade Subjected to Midchord Torsional Oscillation at High Subsonic Stall Flutter Conditions," NASA TM-78998, 1978.

[3] Wuerker, R. F., Kobayashi, R. J., Heflinger, L. O., and Ware, T. C., "Application of Holography to Flow Visualization Within Rotating Compressor Blade Row," AiResearch Mfg. Co., Los Angles, Rept. AIRESEARCH-73-9489, Feb. 1974 (also NASA CR-121264).

[4] Strazisar, A. J. and Chima, R. V., "Comparison Between Optical Measurements and a Numerical Solution of the Flow Field in a Transonic Axial-Flow Compressor Rotor," AIAA Paper 80-1078, June 1980.

[5] Decker, A. J., "Holographic Flow Visualization of Time-Varying Shock Waves," *Applied Optics*, Vol. 20, No. 18, Sept. 1981, pp. 3120-3127.

AIAA 82-4191

# "Coriolis Resonance" within a Rotating Duct

M. Kurosaka* and J. E. Caruthers†
*University of Tennessee Space Institute, Tullahoma, Tenn.*

CURIOUSLY enough, although investigations[1] on unsteady disturbances in axial flow compressors abound, little appears to be available in the open literature for centrifugal machines. However, the flow-induced vibration problems in centrifugal compressors are no less frequent or harassing than their axial-flow counterparts.

In contrast to the axial-flow compressors, in the radial-flow machines we expect the Coriolis force to exert dominating effects upon the unsteady disturbances. For one thing, the Coriolis force more closely couples the disturbances in two flow directions: the radial and circumferential directions. For another—and more important—when we recall that a) the Coriolis force is proportional to twice the shaft-rotation frequency ($2\Omega$) and b) the time-derivative terms of the equation of motion are proportional to the frequency of flow disturbances ($\omega$), there looms an intriguing possibility that a resonance might occur at $\omega=2\Omega$. To the extent that the aforementioned dynamic coupling in two flow directions exists, such a resonance would be akin to the one in the mechanical vibration of a two-degree-of-freedom system. Aside from this, from the aeroacoustic point of view, the pronounced effect of rotation may alter markedly the cut-off condition.

To explore these questions and to do so without being entangled in encumbering analysis, we pose a simple, model problem: an investigation into unsteady disturbances with frequency $\omega$ within a radial duct, which rotates with angular speed $\Omega$ about the $z$ axis (Fig. 1). In the absence of unsteady disturbances, the steady velocity $u_0$ is directed toward the radial direction; the height of the duct in the $z$ direction is uniform.

We assume that the flow is compressible, inviscid and the fluid is a perfect gas. We take the coordinate system fixed to the rotating duct and separate the unsteady part, denoted by primes, from the base, steady part with subscript *0*

$$u_r=u_0+u', \quad u_\theta=v', \quad u_z=w'$$

$$p=p_0+p', \quad \rho=\rho_0+\rho', \quad s=s_0+s' \tag{1}$$

where $s$ is the entropy, the other notation being standard. By substituting Eq. (1) into the governing equations, written in cylindrical coordinates, and neglecting the second-order terms in disturbances, we obtain, as usual, two sets of equations: one for the steady part and the other for unsteady disturbances, the latter being of our central interest.

We further assume the following: 1) the wavelength of the unsteady disturbances in the radial direction is small compared to the radial length of the duct; 2) $u_0$ does not vary in the $\theta$ and $z$ directions; 3) $p_0$, $\rho_0$, and $a_0$ (acoustic speed) do not vary in the $z$ direction; 4) $2\Omega r\Theta/u_0 \ll 1$, when $\Theta$ shown in Fig. 1 is the half-angle of the duct; and 5) $s_0$ is a constant. On the assumption of point 4 the derivatives of the steady parts in the radial direction are small compared to the variation of the unsteady disturbances in the same direction; for example,

$$\frac{\partial p_0}{\partial r} \ll \frac{\partial p'}{\partial r}$$

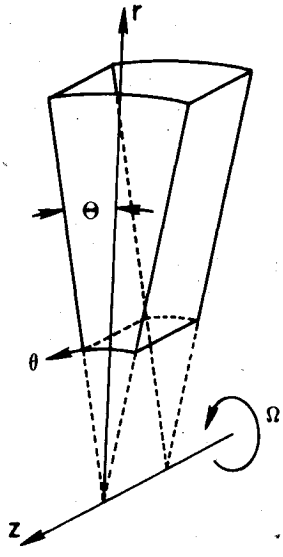


**Fig. 1 Radially divergent rotating duct.**

Received Sept. 4, 1981; revision received Dec. 11, 1981. 

*Professor of Aerospace and Mechanical Engineering. Associate Fellow AIAA.

†Associate Professor of Engineering Science and Mechanics.

and the like; therefore such steady derivatives are negligible in comparison to their unsteady counterpart. Assumption 4 is a slender duct approximation and can be shown, along with assumption 5, to yield the results that $p_0$, $\rho_0$, and $a_0$ do not vary in the $\theta$ direction. Combined with assumption 3, this implies that $p_0$, $\rho_0$, and $a_0$ can be treated as constants.

All of this leads to the following set of equations for the unsteady disturbances

$$\frac{\partial \rho'}{\partial t} + u_0 \frac{\partial \rho'}{\partial r} + \rho' \frac{u_0}{r} + \rho_0 \left( \frac{u'}{r} + \frac{\partial u'}{\partial r} + \frac{1}{r} \frac{\partial v'}{\partial \theta} + \frac{\partial w'}{\partial z} \right) = 0 \tag{2a}$$

$$\frac{\partial u'}{\partial t} + u_0 \frac{\partial u'}{\partial r} = -\frac{a_0^2}{\rho_0} \frac{\partial \rho'}{\partial r} + 2\Omega v' \tag{2b}$$

$$\frac{\partial v'}{\partial t} + u_0 \frac{\partial v'}{\partial r} + \frac{u_0 v'}{r} = -\frac{a_0^2}{\rho_0 r} \frac{\partial \rho'}{\partial \theta} - 2\Omega u' \tag{2c}$$

$$\frac{\partial w'}{\partial t} + u_0 \frac{\partial w'}{\partial r} = -\frac{a_0^2}{\rho_0} \frac{\partial \rho'}{\partial z} \tag{2d}$$

In the preceding, $u_0$ is, as far as the unsteady disturbances are concerned, only slowly varying in the radial direction from the assumption of 1, and as such, we regard it as constant. The last terms on the right-hand sides of Eqs. (2b) and (2c) represent, of course, the components of the Coriolis force.

We express the unsteady disturbances by Fourier decomposition in $\theta$, $z$, and $t$ so that $u'$, $v'$, $w'$, and $\rho'$ all take the form of $\exp[i(m\theta + kz - \omega t)]$. In addition, we restrict our attention to the solution of Eq. (2) at large values of $r$ and let

$$\begin{bmatrix} u' \\ v' \\ w' \\ \rho' \end{bmatrix} \sim \begin{bmatrix} A \\ B \\ C \\ D \end{bmatrix} r^{-1/2} \exp[i(\ell r + m\theta + kz - \omega t)] \tag{3}$$

where $A$, $B$, $C$, and $D$ are the amplitudes of $u'$, $v'$, $w'$, and $\rho'$ respectively; they are to be determined from Eq. (2). The aforementioned radial dependence in the form of $r^{-1/2}\exp(i\ell r)$ is motivated by the asymptotic expression of the Hankel function of the first kind, which is a solution of Eq. (2) when $u_0 = 0$ and takes such a form when $\ell r \gg 1$.

Substitution of Eq. (3) into Eq. (2) yields

$$A = -\frac{\lambda \ell}{(2\Omega)^2 - \lambda^2} \frac{a_0^2}{\rho_0} D \tag{4a}$$

$$B = \frac{i 2\Omega \ell}{(2\Omega)^2 - \lambda^2} \frac{a_0^2}{\rho_0} D \tag{4b}$$

$$C = \frac{1}{\lambda} \frac{a_0^2}{\rho_0} kD \tag{4c}$$

$$\lambda^4 - \lambda^2 [(2\Omega)^2 + a_0^2 (k^2 + \ell^2)] + (2a_0 k\Omega)^2 = 0 \tag{4d}$$

where $\lambda = \omega - u_0 \ell$. The appearance of $\omega$ and $u_0$ in the combined form of $\lambda$ embodies, of course, the Doppler shift.

In the amplitudes of the radial and tangential disturbances, $A$ and $B$, the denominators immediately reveal the possibility of resonance at $2\Omega = \lambda$. Substitution of this into Eq. (4d) yields that at such a condition $\ell$ becomes zero; then, from the definition of $\lambda$, $2\Omega = \lambda$ corresponds to $2\Omega = \omega$. Since $\ell$ appears in the numerators of $A$ and $B$, we examine the behavior of Eqs. (4a) and (4b) near $2\Omega = \omega$. A simple calculation leads to the following approximation, valid near $2\Omega = \omega$:

$$A \sim \frac{2\Omega - (a_0 k)^2 (2\Omega)^{-1}}{\omega - 2\Omega} u_0 \frac{D}{\rho_0} \tag{5a}$$

$$B \sim -\frac{2\Omega - (a_0 k)^2 (2\Omega)^{-1}}{\omega - 2\Omega} i u_0 \frac{D}{\rho_0} \tag{5b}$$

These, indeed, display the resonance at $\omega = 2\Omega$, as expected. In contrast to the resonance of the radial and circumferential disturbances, the amplitude of the axial disturbance, Eq. (4c), does not exhibit such a behavior. Nor does it increase when the denominator $\lambda$ tends to zero, since at the conditions $k$ is shown to decrease equally fast, leaving $C$ finite.

Only the radial and circumferential disturbance resonate at $\omega = 2\Omega$ and this reflects the fact that the phenomenon is induced by the Coriolis force, whose components are present only in these two directions; hence, we call it the "Coriolis resonance." The Coriolis force plays the role of an "external excitation force" with frequency $2\Omega$ and resonance sets up when the "natural frequency" $\omega$ of the unsteady disturbances coincides with $2\Omega$.

Near resonance, the wavenumber in the radial direction is shown to become

$$\ell \sim (\omega - 2\Omega)/u_0 \tag{6}$$

This indicates that as $\omega$ approaches $2\Omega$, the rate of the sinusoidal variation in the radial direction, $\exp(i\ell r)$, becomes slower and slower. Then, when we look at Eq. (3) and focus attention to their radial dependence only, we find that the unsteady disturbances vary essentially like $\bar{r}^{1/2}$: the usual two-dimensional decay caused by their spreading in the $r$ direction, the sinusoidal fluctuation term, $\exp(i\ell r)$, becoming almost constant. Although we cannot carry this too far, because of the formal restriction of $\ell r \gg 1$, not to mention the breakdown of the linearized approximation at the resonance, still the trend toward slower oscillation in the radial direction appears to be a correct one. The reason is as follows.

For an incompressible, rotating fluid with no base flow, Görtler[2] showed that the fundamental characteristics of flow change drastically, depending on the competition between $\omega$ and $2\Omega$. For $\omega > 2\Omega$, the flowfield is elliptic; when $\omega < 2\Omega$ it is hyperbolic. The situation is strikingly analogous to compressible, nonrotating flow and, in fact, for $\omega < 2\Omega$, a "Mach cone" with its axis aligned in the $z$ direction, the axis of rotation, appears even within an *incompressible* flow, as demonstrated experimentally by Görtler[3] (see also, Greenspan[4]). Here, the Mach cone angle is equivalent to the one corresponding to the Mach number $M = 2\Omega/\omega$. Viewed from this point, the Taylor-Proudman flow, with $\omega = 0$, corresponds to the "hypersonic" limit.

Even for a compressible, rotating flow, with still no base flow, we easily can show that the situation remains the same; the Mach number being given again by $M = 2\Omega/\omega$. Then, the Coriolis resonance condition, $2\Omega = \omega$, corresponds to the "transonic" flow, $M = 1$. Just like ordinary transonic flow, if we change only the radial position, here at resonance the sinusoidal disturbance in the rotating flow at one point will be felt unchanged at another point, except for the spatial decay of $\bar{r}^{1/2}$. This appears to be the reason for the aforementioned waning of the sinusoidal spatial dependence near resonance; although in the present problem the base flow $u_0$ is present, its effect seems to become lessened near resonance when its multiplying factor $\ell$ becomes smaller.

The possible existence of the Coriolis resonance appears to be peculiar to an open-ended duct such as that in centrifugal compressors, since the presence of an end wall of any closed duct would certainly prevent it.

We now leave the issue of Coriolis resonance and turn to the question of the cut-off condition. By imposing a

requirement that $\ell$ in Eq. (4d) should be real, we obtain, after some lengthy but straightforward algebra,

$$k^2 \le \frac{\omega^2}{a_0^2-u_0^2}+\left(\frac{2\Omega}{a_0}\right)^2\left[-1+\left(\frac{a_0k}{\omega}\right)^2(1-M_0^2)^2 + \left(\frac{2\Omega}{\omega}\right)^2 M_0^2\left(\frac{a_0k}{\omega}\right)^4(1-M_0^2)^5+O\left(\frac{2\Omega}{\omega}\right)^3\right] \quad (7)$$

where $M_0=u_0/a_0$; the expression is valid for $2\Omega/\omega \ll 1$, or below Coriolis resonance. On the right-hand side of the inequality just given, the second term represents the effect of rotation, which, obviously, is absent for a nonrotating duct.

The confirmation of the present predictions, either by elaborate numerical procedure or experiments, remains to be settled.


## Acknowledgments

The work is supported by NASA Lewis Research Center, under Contract NASA NAG 3-86 with Dr. W. Rostafinsky as a technical monitor.


## References


[1] Goldstein, M. E., *Aeroacoustics*, McGraw-Hill Book Co., New York, 1976.

[2] Görtler, H., "Einige Bemerkungen über Strömungen in rotierenden Flüssigkeiten," *Zeitschrift der Angewandte Mathematik und Mechanik*, Vol. 24, No. 5, 1944, pp. 210-214.

[3] Görtler, H., "On Forced Scillations in Rotating Fluids," *Proceedings of the Fifth Midwestern Conference on Fluid Mechanics*, University of Michigan Press, Ann Arbor, Mich., 1957, pp. 1-10.

[4] Greenspan, H. P., *The Theory of Rotating Flows*, Cambridge University Press, Cambridge, England, 1968, p. 3.


---

AIAA 82-4192

# Pressure Distributions and Shock Shapes for a Bent-Nose Biconic at Incidence


Charles G. Miller III* and Peter A. Gnoffo*

*NASA Langley Research Center, Hampton, Va.*


## Nomenclature

$L$ = model length, m
$N_{Re}$ = unit Reynolds number, $m^{-1}$
$p$ = pressure, $N/m^2$
$y,z$ = coordinates (see Fig. 1)
$\alpha$ = angle of attack, deg
$\theta$ = cone half angle, deg
$\phi$ = circumferential angle, deg ($\phi=180$ deg is most windward ray and $\phi=0$ deg is most leeward ray)

*Subscripts*

$f$ = fore cone
$m$ = measured
$\infty$ = freestream conditions
$s$ = surface

Received Sept. 3, 1981; revision received Dec. 9, 1981. This paper is declared a work of the U.S. Government and therefore is in the public domain.

*Aero-Space Technologist, Aerothermodynamics Branch, Space Systems Division. Member AIAA.

## Introduction

FEASIBILITY studies of the aerocapture and aerobraking techniques[1-3] for proposed flights to Mars, Venus, Saturn, and Titan demonstrate that the biconic shape offers the best combination of high lift-to-drag ratio for inserting accuracy, low hypersonic ballistic coefficient, and high volumetric efficiency. Also, biconic shapes would fit nicely into the shuttle orbiter bay. The leading candidate emerging from these feasibility studies[2,3] is a 12.84/7 deg biconic with the fore-cone section bent upward relative to the aft-cone section. To assist in the establishment of an accurate hypersonic data base for this proposed configuration, a study has been initiated at the Langley Research Center. The purpose of this Note is to present the initial results of this experimental study and make comparisons to prediction. These results include pressure distributions and shock shapes measured on a spherically blunted bent-nose biconic model at Mach 6 in air for angles of attack from 0 to 25 deg.

## Apparatus and Tests

The present study was performed in the Langley 20-in. Mach 6 tunnel.[4] Reservoir pressure and temperature were 3.5 $MN/m^2$ and 500 K, respectively, corresponding to a freestream Mach number of 6.0 and unit Reynolds number of $28.7\times10^6$/m in ideal air.

A planform view of the bent-nose biconic model is shown in Fig. 1. This model has a fore-cone half-angle of 12.84 deg, aft-cone half-angle of 7 deg, spherical nose radius of 5.79 mm, and base radius of 3.81 cm. The fore cone is bent upward 7 deg relative to the aft cone. Sixty-two surface pressure orifices were distributed along five rays (the most windward, most leeward, and three rays at 45-deg increments between the windward and leeward rays) and two orifices were located on the base. The model was mounted with a 2.54-cm-diam sting and the ratio of sting length to diameter exceeded 7. Tests were performed over a range of angle of attack $\alpha$ from 0 to 25 deg in 5-deg increments, where $\alpha$ is referenced to the axis of the aft-cone section. The angle of attack was read from the schlieren photographs.

Pressures were measured using variable capacitance diaphragm transducers and the output recorded by an analog-to-digital system. Shock shapes were recorded using a single pass schlieren system. These shock shapes were read manually from enlargements of schlieren photographs to approximately 1.4 times actual model size.

## Prediction

Pressure distributions and shock shapes were computed using a steady, three-dimensional, inviscid flowfield code.[5] This code, referred to as STEIN (supersonic three-dimensional external inviscid), uses a MacCormack-like scheme to integrate the three-dimensional Euler equations. Shock waves are computed as discontinuities via the Rankine-Hugoniot jump conditions. The Mach number in the marching direction (an axis running from the nose of the vehicle to the base) must be supersonic at every point in the flowfield, and the geometry such that no embedded regions of subsonic flow exist. The subsonic-supersonic flow about the spherical nose was computed using a blunt body code.[6]

## Results and Discussion

Measured and predicted shock shapes are presented in Fig. 1 for various angles of attack. The most upstream inflection in the measured windward shock is due to an overexpansion of the flow from the spherical nose.[7] The second inflection on the windward side is due to the flow expansion occurring at the fore-cone/aft-cone junction. The point at which the windward shock turns inward due to the junction moves slowly toward the nose with angle of attack. For $\alpha_m \ge 21$ deg, the windward shock just upstream of the base has become parallel to the aft-cone surface. Shock detachment distance on